ARTICLE

www.the-innovation.org

A midgut transcriptional regulatory loop favors an insect host to withstand a bacterial pathogen

Zhaojiang Guo,[1,5,*] Liuhong Zhu,[1,5] Zhouqiang Cheng,[1,5] Lina Dong,[1,5] Le Guo,[1,5] Yang Bai,[1,5] Qingjun Wu,[1] Shaoli Wang,[1] Xin Yang,[1] Wen Xie,[1] Neil Crickmore,[2] Xuguo Zhou,[3] René Lafont,[4] and Youjun Zhang[1,*]

*Correspondence: guozhaojiang@caas.cn (Z.G.); zhangyoujun@caas.cn (Y.Z.)

Received: January 14, 2024; Accepted: July 9, 2024; Published Online: July 14, 2024; https://doi.org/10.1016/j.xinn.2024.100675

© 2024 The Author(s). Published by Elsevier Inc. on behalf of Youth Innovation Co., Ltd. This is an open access article under the CC BY-NC-ND license (http://creativecommons.org/licenses/by-nc-nd/4.0/).

GRAPHICAL ABSTRACT

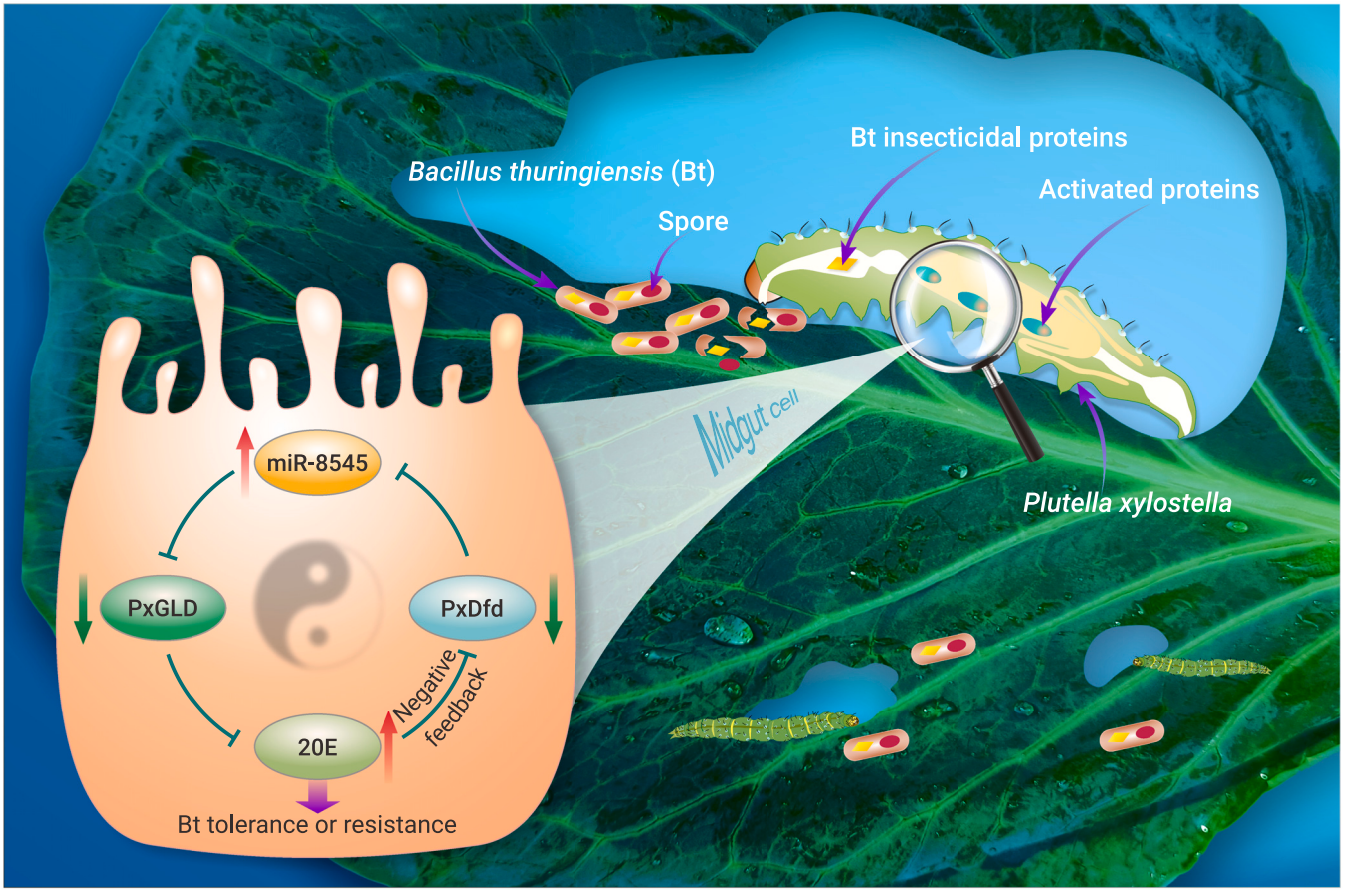

PUBLIC SUMMARY

- Increased titer of the insect hormone 20-hydroxyecdysone (20E) facilitates an insect host, *Plutella xylostella*, to defeat its bacterial pathogen *Bacillus thuringiensis* (Bt).
- Glucose dehydrogenase (GLD) was identified as a new insect ecdysone-degrading enzyme that can metabolize 20E.
- A midgut miRNA initiated epigenetic regulatory pathway represses GLD activity and elevates 20E titer to resist the Bt pathogen.
- An as-yet uncharacterized negative feedback loop reduces excess 20E to balance hormonal homeostasis.
- This study provides new insights into the immunological landscape of classical insect hormones and the molecular basis of host-pathogen coevolution.

ARTICLE

A midgut transcriptional regulatory loop favors an insect host to withstand a bacterial pathogen

Zhaojiang Guo,[1,5,*] Liuhong Zhu,[1,5] Zhouqiang Cheng,[1,5] Lina Dong,[1,5] Le Guo,[1,5] Yang Bai,[1,5] Qingjun Wu,[1] Shaoli Wang,[1] Xin Yang,[1] Wen Xie,[1] Neil Crickmore,[2] Xuguo Zhou,[3] René Lafont,[4] and Youjun Zhang[1,*]

[1]State Key Laboratory of Vegetable Biobreeding, Department of Plant Protection, Institute of Vegetables and Flowers, Chinese Academy of Agricultural Sciences, Beijing 100081, China

[2]School of Life Sciences, University of Sussex, Brighton BN1 9QE, UK

[3]Department of Entomology, School of Integrative Biology, College of Liberal Arts & Sciences, University of Illinois Urbana-Champaign, Urbana, IL 61801-3795, USA

[4]Sorbonne Université, CNRS - IBPS (BIOSIPE), 75005 Paris, France

[5]These authors contributed equally

*Correspondence: guozhaojiang@caas.cn (Z.G.); zhangyoujun@caas.cn (Y.Z.)

Received: January 14, 2024; Accepted: July 9, 2024; Published Online: July 14, 2024; https://doi.org/10.1016/j.xinn.2024.100675

© 2024 The Author(s). Published by Elsevier Inc. on behalf of Youth Innovation Co., Ltd. This is an open access article under the CC BY-NC-ND license (http://creativecommons.org/licenses/by-nc-nd/4.0/).

Citation: Guo Z., Zhu L., Cheng Z., et al., (2024). A midgut transcriptional regulatory loop favors an insect host to withstand a bacterial pathogen. The Innovation **5(5)**, 100675.

Mounting evidence suggests that insect hormones associated with growth and development also participate in pathogen defense. We have discovered a previously undescribed midgut transcriptional control pathway that modulates the availability of 20-hydroxyecdysone (20E) in a worldwide insect pest (*Plutella xylostella*), allowing it to defeat the major virulence factor of an insect pathogen *Bacillus thuringiensis* (Bt). A reduction of the transcriptional inhibitor (PxDfd) increases the expression of a midgut microRNA (miR-8545), which in turn represses the expression of a newly identified ecdysteroid-degrading glucose dehydrogenase (PxGLD). Downregulation of PxGLD reduces 20E degradation to increase 20E titer and concurrently triggers a transcriptional negative feedback loop to mitigate 20E overproduction. The moderately elevated 20E titer in the midgut activates a MAPK signaling pathway to increase Bt tolerance/resistance. These findings deepen our understanding of the functions attributed to these classical insect hormones and help inform potential future strategies that can be employed to control insect pests.

INTRODUCTION

For over a century, insect endocrinologists have known about two non-peptide hormones, juvenile hormone (JH), and 20-hydroxyecdysone (20E), which collaboratively govern fundamental life-history traits including growth, development, and reproduction in insects.[1-4] Furthermore, it has more recently been reported that these pleiotropic hormones can also orchestrate insect defenses against pathogenic infections.[5,6] While this hormone-triggered pathogen defense is of paramount importance for insect survival, the molecular control mechanisms are poorly understood.

Bacillus thuringiensis (Bt) is a Gram-positive entomopathogenic bacterium that produces various insecticidal toxins, which upon ingestion destroy the midgut epithelium of its insect host.[7,8] This destruction is an essential step in the pathogenicity of the bacterium, as it allows its spore to enter the insect and initiate septicemia.[9] Bt pore-forming toxins exert their virulence by initially binding to specific midgut receptors, such as cadherin, alkaline phosphatase (ALP), aminopeptidase N (APN), and ATP-binding cassette (ABC) transporters.[10-13] Bioinsecticides and transgenic Bt crops reliant on the insecticidal activity of Bt toxins have become the most successful agricultural biotechnology products for insect pest control.[14-17] Nonetheless, it has been reported that more than 13 agricultural pests have evolved practical resistance to these products, seriously threatening the sustainable use of Bt-based technologies.[18-21]

The diamondback moth, *Plutella xylostella* (L.) was the first insect pest discovered to have developed high-level resistance to Bt bioinsecticides in open fields,[22] making it a suitable model to study the underlying molecular regulatory network affecting host-pathogen interactions.[23] Recently, our studies have found that an elevated level of the insect hormone 20E can upregulate the expression of MAP4K4 to activate a four-tiered MAPK signaling cascade, resulting in a decrease in expression of different midgut receptors (ALP, APN1, APN3a, ABCB1, ABCC2, ABCC3, and ABCG1) and an increase in the expression of non-receptor paralogs (APN5, APN6, and ABCC1) to thwart the virulence effect of the Bt Cry1Ac toxin.[6,24-34] Although we demonstrated the critical role of an increased 20E titer in the Bt tolerance/resistance phenotype, the underlying regulatory mechanism was obscure.[6]

In this study, we wanted to gain a deeper insight into how a major insect pest regulates an effective pathogen defense via a pathway involving a hormone classically associated with growth and development. Such knowledge cannot only potentially inform the design of future pest control strategies, but also expand our understanding of the pleiotropic roles of classic hormones during the normal feeding stage of an insect larva.

RESULTS

miRNA biogenesis response to Bt intoxication in *P. xylostella*

To decipher whether miRNA biogenesis might affect the tolerance or resistance to Bt Cry1Ac toxin in *P. xylostella*, we first identified and cloned the *PxDcr-1* gene from *P. xylostella* midgut tissues via five overlapping gene-specific fragments (Figures S1A and S1C; Table S2). The obtained full-length cDNA sequence of *PxDcr-1* (GenBank accession no. OR130726) is 8,601 bp in length, contains 41 exons (Figure S1B), and the encoded protein carries 6 conserved ribonuclease Dcr-1 domains (Figure S1D). Phylogenetic analyses illustrated that PxDcr-1 is evolutionarily conserved and is clustered with the Lepidoptera branch (Figure S1E). Spatiotemporal gene expression analysis showed that *PxDcr-1* was abundantly expressed in the head, and at the egg and pupa stages (Figures S2A and S2B). After treating susceptible DBM1Ac-S larvae with 1 mg/L (LC_{50}) or 2 mg/L (LC_{90}) of Cry1Ac protoxin, the expression level of *PxDcr-1* was induced in midgut tissues (Figure S2C). The expression level of *PxDcr-1* was also greater in the midgut tissues of the Cry1Ac-resistant NIL-R strain than in the susceptible DBM1Ac-S strain (Figure S2D).

To further unravel the possible role of *PxDcr-1* in Bt Cry1Ac resistance, we silenced *PxDcr-1* expression by microinjecting a sublethal dose of specific siPxDcr-1 (30 μM) into early third-instar larvae from the Cry1Ac-resistant NIL-R strain. Toxicity and qPCR assays confirmed the knockdown of *PxDcr-1* and showed a significantly increased susceptibility to 1,000 mg/L Cry1Ac (Figures S2E and S2F). These results suggested that miRNA-mediated epigenetic modulations might participate in Cry1Ac tolerance/resistance in *P. xylostella*.

miR-8545 mediates Cry1Ac resistance

To identify functional miRNAs involved in Cry1Ac tolerance/resistance, we conducted high-throughput sequencing of small RNAs using midgut tissues from Cry1Ac-susceptible DBM1Ac-S and Cry1Ac-resistant NIL-R strains. Overall, 74 million high-quality reads were obtained (Table S1) and a total of 363 miRNAs, including 173 known and 190 new miRNAs, were identified (Figure S3A; Tables S5 and S6). The size distribution of the miRNAs was primarily in the range of 20–23 nt (Figure S3B). Previous studies have shown that the dominance of uracil at the first position of the 5′ end is considered a defining feature of mature miRNAs, as this base facilitates the interaction between miRNAs and Argonaute complexes.[35] We found that the first nucleotide of our identified mature miRNAs was biased toward uracil (U) (Figure S3D). Among these miRNAs, 44 (7 known and 37 novel) were found to be differentially expressed between the two strains (Figure 1A; Table S7). The 7 known miRNAs were cloned by reverse-transcription PCR (Figure S3C), and

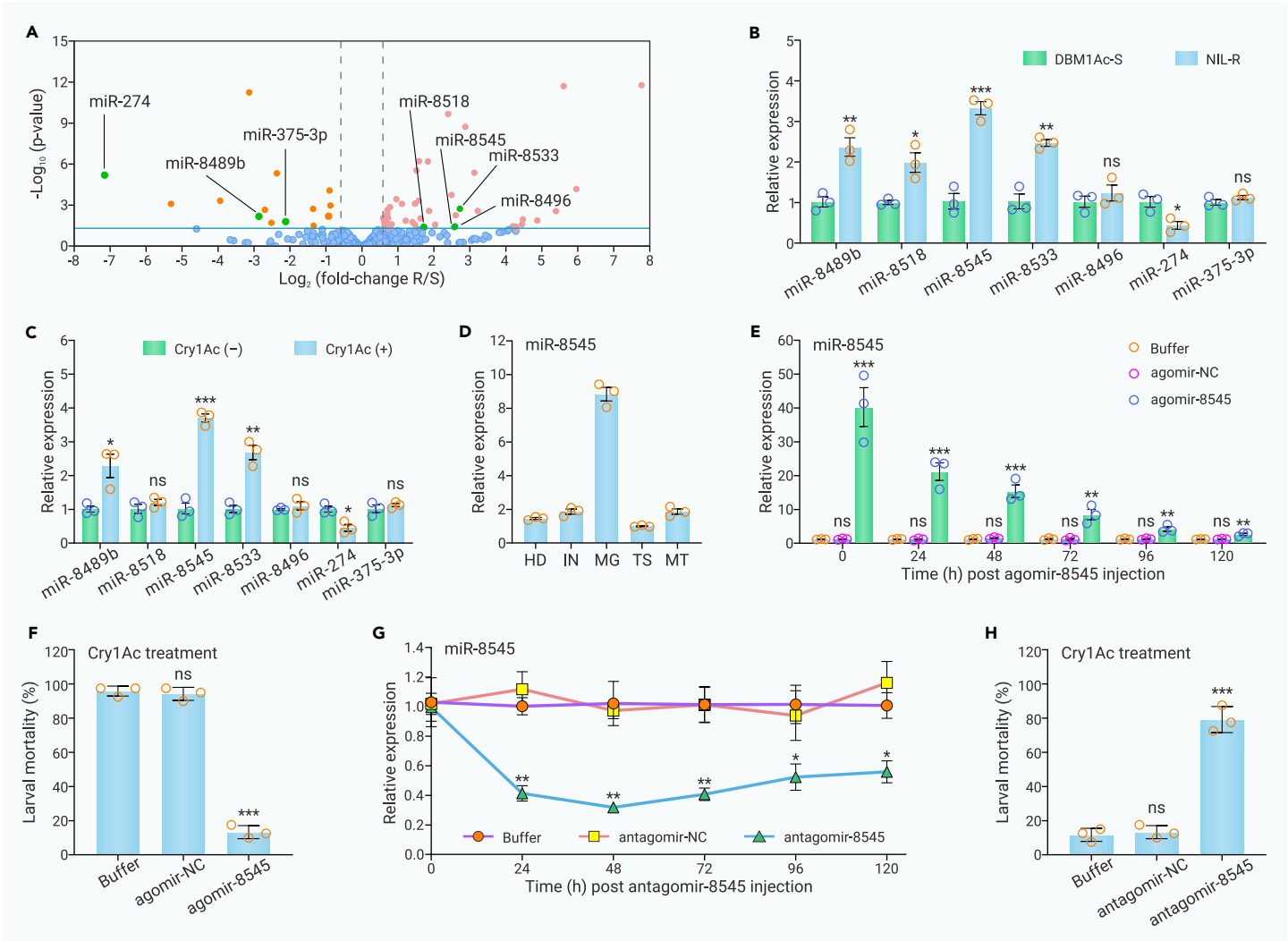

Figure 1. Overexpression of midgut miR-8545 enhances Bt Cry1Ac resistance in *P. xylostella* (A) Volcano map of miRNA expression changes in the midgut of susceptible DBM1Ac-S and resistant NIL-R strains, each dot indicates an individual miRNA. Average miRNA expression level from three biological repeats (transformed to log2 scale) was graphed against *p* value by Student's t-test (transformed to −log10 scale). Green and gray lines were used to respectively denote the cutoff of $p = 0.05$ and 1.5-fold change. The strikingly altered known miRNAs ($p < 0.05$, fold change > 1.5) are emphasized in green. (B) miRNA transcript levels in the larval midgut of Bt Cry1Ac-susceptible DBM1Ac-S and Cry1Ac-resistant NIL-R strains. (C) Effects of an LC_{50} Cry1Ac protoxin concentration (1 mg/L) on the expression levels of the seven known miRNAs in the susceptible strain. (D) The relative transcript levels of miR-8545 in various larval tissues including head (HD), integument (IN), midgut (MG), testis (TS), and Malpighian tubules (MT). (E and F) Effect of microinjecting agomir-8545 on miR-8545 transcript level (E) and larval mortality (treated by 2 mg/L (LC_{90}) Cry1Ac protoxin) (F) in the susceptible DBM1Ac-S strain. (G and H) Effect of microinjecting antagomir-8545 on miR-8545 transcript level (G) and larval mortality (treated with 1,000 mg/L (LC_{10}) Cry1Ac protoxin) (H) in the resistant NIL-R strain. *U6* was utilized as the internal reference gene, and the transcript levels in the susceptible (B), the Cry1Ac-untreated (C), the lowest expressed DBM1Ac-S samples (D) and the buffer-treated susceptible DBM1Ac-S (E) and resistant NIL-R samples (G) were set to 1. Bars are mean ± SEM (B–H). ns, not significant; $*p < 0.05$, $**p < 0.01$, $***p < 0.001$; one-way ANOVA adjusted by Tukey's test.

subsequent qPCR expression analysis confirmed that 5 were differentially expressed between midguts of the susceptible and resistant strains (Figure 1B), and 4 were identified to be differentially expressed in larvae of the susceptible strain 72 h after exposure to an LC_{50} (1 mg/L) concentration of Cry1Ac protoxin (Figure 1C). We noted that miR-8545 had the most significant differences in the above two conditions.

Tissue expression profiles showed that miR-8545 was highly enriched in the midgut tissues of *P. xylostella* (Figure 1D). To further explore whether the increased expression of miR-8545 was related to Cry1Ac resistance, the miR-8545 concentration in susceptible DBM1Ac-S larvae was increased by microinjecting a miR-8545 mimic (agomir-8545) (Figure 1E). Toxicity bioassays conducted at 72 h post-injection revealed that this increase in miR-8545 substantially reduced Cry1Ac susceptibility at 2 mg/L (LC_{90}) compared with the controls (Figure 1F). Conversely, inhibition of miR-8545 was performed in the resistant NIL-R strain via injection of antagomir-8545 (Figure 1G). Bioassay results demonstrated that antagomir-8545 injection increased Cry1Ac susceptibility at 1,000 mg/L (LC_{10}) (Figure 1H). These results indicated that miR-8545 could be a crucial factor mediating the response to Cry1Ac in *P. xylostella*.

miR-8545 binds to a *PxGLD* gene

To decipher the molecular mechanism by which miR-8545 might regulate Cry1Ac susceptibility in *P. xylostella*, we employed five software programs, namely miRanda, PITA, RNA22v2, RNAhybrid, and RIsearch2, to predict the potential targets of miR-8545. These identified seven genes as strong candidates (Figure 2A). Expression analysis found that two of these, obstructor-E (*PxObst-E*) and *PxGLD*, were differentially expressed in the midgut tissues of Cry1Ac-susceptible DBM1Ac-S and Cry1Ac-resistant NIL-R larvae (Figure 2B). *PxGLD* was also found to be abundantly expressed in midgut tissues based on our previous midgut transcriptome data of *P. xylostella*[36] (Figure 2B).

To further investigate these two potential miR-8545 targets, we performed luciferase assays in human HEK293T cells (Figure 2C). Only luciferase activity from the construct containing *PxGLD* was significantly decreased by miR-8545 (Figure 2D). Mutations in the miRNA binding site of *PxGLD* (Figure S3E) eliminated the suppressive effects of miR-8545 (Figure 2D). If miR-8545 binds to *PxGLD in vivo*, they will form a functional RNA-induced silencing complex with AGO1 protein, so we then performed RNA immunoprecipitation assays from midgut tissues using *P. xylostella*-specific AGO1 antibody as a means of validating the function of this miRNA.[37] The results demonstrated that

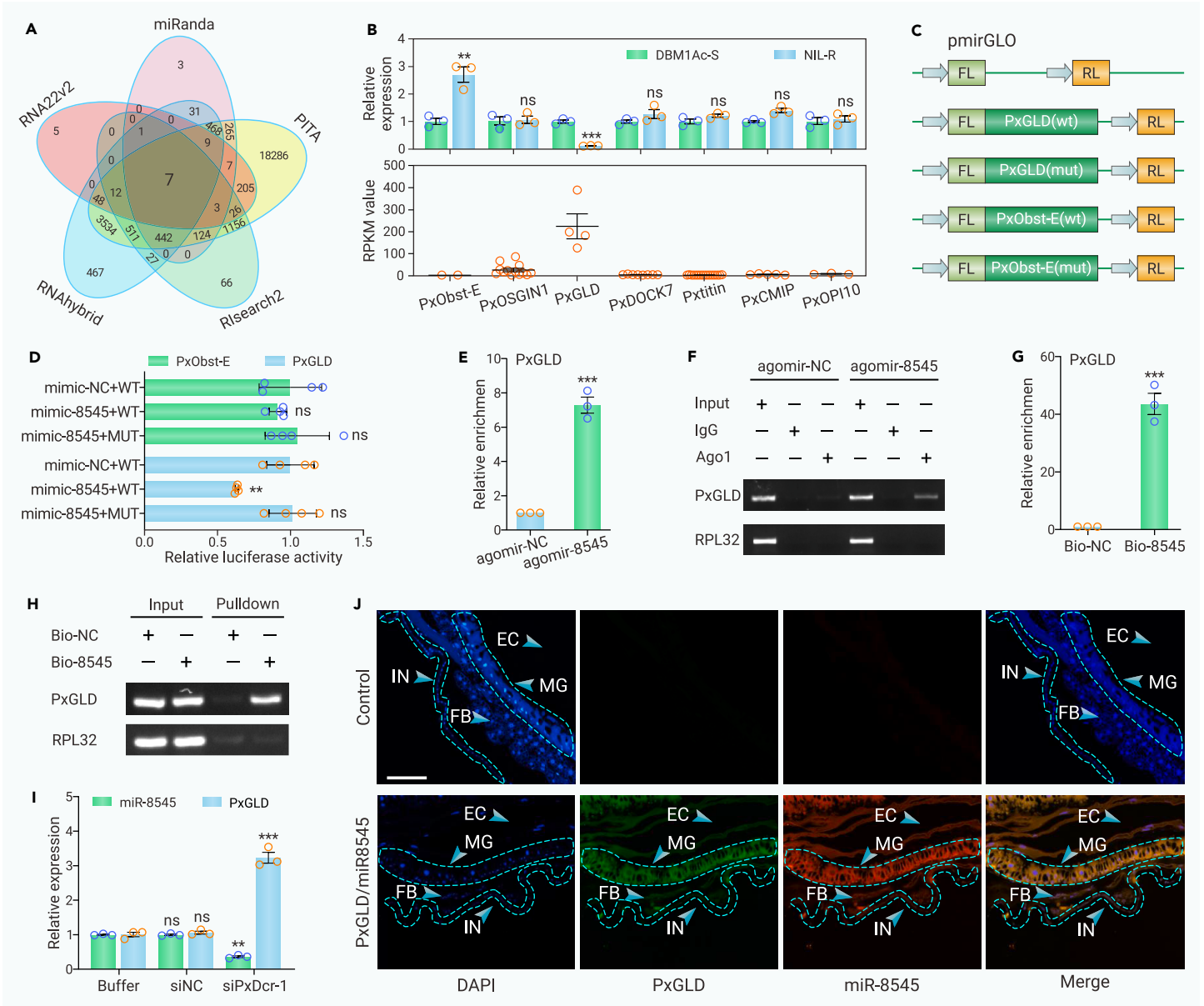

Figure 2. *PxGLD* is identified as a direct target of miR-8545 (A) The potential targets of miR-8545 were predicted through five software algorithms (miRanda, PITA, RISearch2, RNAhybrid, and RNA22v2). (B) The upper panel shows the transcription levels of seven potential target genes in the larval midgut of Bt Cry1Ac-susceptible DBM1Ac-S and Cry1Ac-resistant NIL-R strains. The lower panel shows the absolute expression of the seven potential genes in our previously built midgut transcriptome and RNA-seq library of DBM1Ac-S larvae. (C) Luciferase reporter constructs. The dual reporter vector pmirGLO expresses firefly luciferase (FL) and Renilla luciferase (RL) under their respective promoters. The empty vector pmirGLO is used as a control. The plasmid pmirGLO-PxGLD/PxObst-1 (WT) has the PxGLD/PxObst-1 CDS with its miR-8545 binding site directly inserted after the FL coding region. The plasmid pmirGLO-PxGLD/PxObst-1 (mut) has the PxGLD/PxObst-1 CDS with a mutation in the miR-8545 binding site. (D) Luciferase reporter assays in HEK293T cells co-transfected with mimic-8545/mimic-NC and pmirGLO vectors. The co-transfection of mimic-NC/WT was used as a control and the value was set to 1. (E and F) RNA immunoprecipitation assay conducted with specific anti-Ago-1 antibody. RT-qPCR (E) and RT-PCR (F) assays were carried out to amplify the *PxGLD* gene from the Ago-1 enrichment group after microinjection with agomir-8545 or agomir-NC. The agomir-NC-treated group was used as a control and the value was set to 1. (G and H) RNA pull-down assay performed 48 h after microinjection of biotinylated miR-8545 (bio-8545) or a poly(A) RNA sequence (bio-NC) into *P. xylostella* larvae. RT-qPCR (G) and RT-PCR (H) were used to analyze *PxGLD* mRNA from the immunoprecipitates, and the bio-NC-treated group was used as a control and the value was set to 1. (I) Effect of *PxDcr-1* silencing on the expression levels of miR-8545 and *PxGLD* in the larval midguts. The buffer-treated strain was set to 1. (J) Co-localization of miR-8545 and *PxGLD* in the midgut. *PxGLD* and miR-8545 were labeled with FAM (green) and Cy3 (red), respectively. A yellow signal is obtained in the midgut when the green (*PxGLD*) and red signals (miR-8545) overlap, indicating the co-localization of *PxGLD* and miR-8545. The images were captured using a Nikon Eclipse Ci fluorescence microscope. Scale bar, 50 μm. IN, integument; MG, midgut; FB, fat body; EC, enteric cavity. Bars are mean ± SEM (B, D, E, G, and I). ns, not significant; *$p < 0.05$, **$p < 0.01$, ***$p < 0.001$; one-way ANOVA adjusted by Tukey's test.

PxGLD was enriched in the agomir-8545-injected group compared with the agomir-NC-injected negative control group (Figures 2E and 2F). *PxGLD* was also significantly enriched in a biotin-labeled miR-8545 pull-down fraction compared with the negative Bio-NC fraction in an RNase-assisted RNA pull-down assay (Figures 2G and 2H). Furthermore, we tested whether knockdown of *PxDcr-1* would affect the transcript levels of miR-8545 and *PxGLD*. While the expression levels of mature miR-8545 were silenced, the transcript levels of *PxGLD* were greatly elevated in larvae treated with a sublethal dose (30 μM) of specific siPxDcr-1 (Figure 2I). A fluorescence *in situ* hybridization assay was then conducted to further probe the interaction between miR-8545 and *PxGLD*. The results indicated that miR-8545 and *PxGLD* co-localized in the midgut tissues (Figure 2J). The above results are all indicative of a direct interaction between miR-8545 and *PxGLD* in the midgut of *P. xylostella*.

Downregulation of *PxGLD* is linked to Cry1Ac resistance

To explore whether the miR-8545-induced tolerance/resistance to Cry1Ac is mediated through *PxGLD*, we first cloned the full-length cDNA sequence of the *PxGLD* gene (GenBank accession no. OR130727) (Figure S4A). Phylogenetic analysis found that PxGLD is clearly clustered with the Lepidoptera group, and indicates that the *PxGLD* gene is evolutionarily conserved within diverse insect

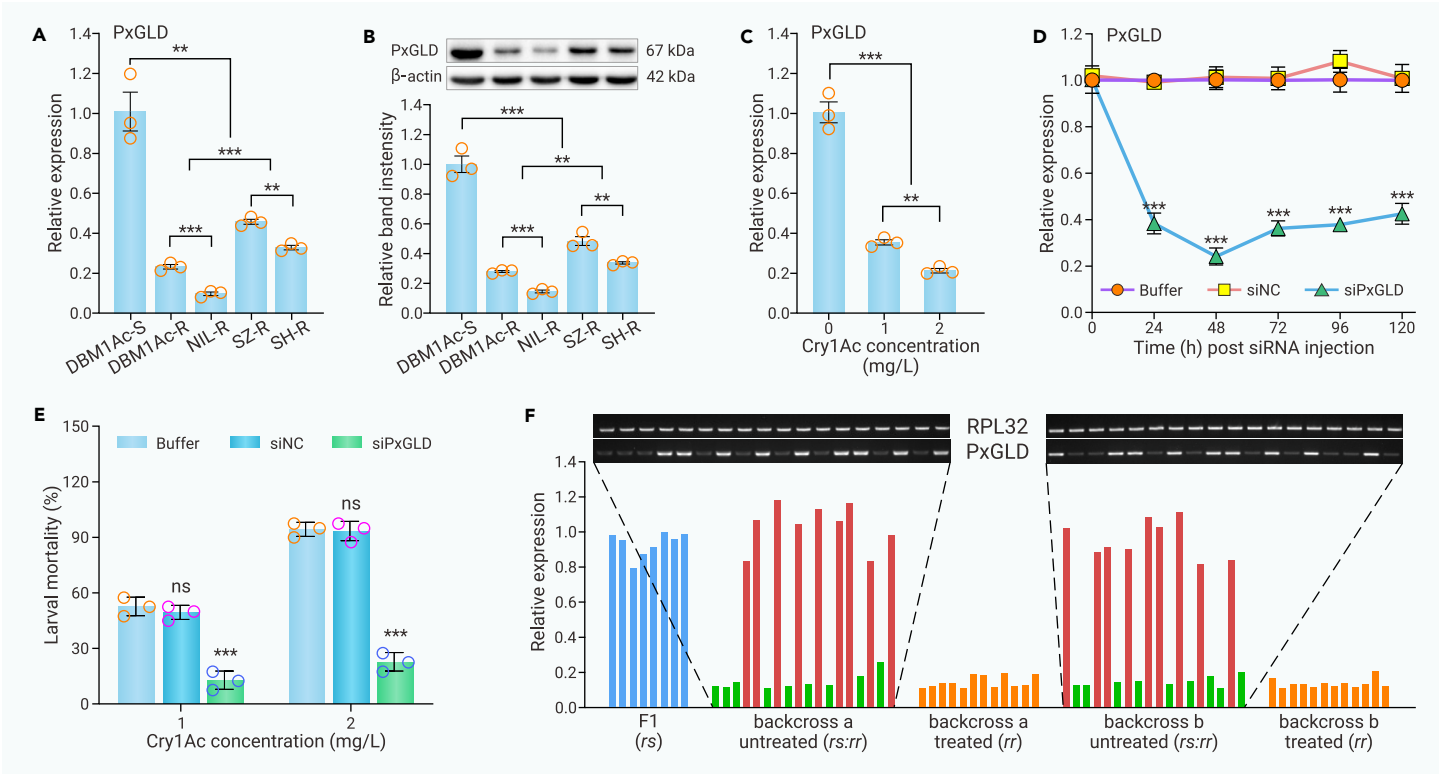

Figure 3. Decreased expression of the midgut *PxGLD* is linked to Cry1Ac resistance phenotype (A and B) The transcript (A) and protein (B) levels of *PxGLD* in the midgut tissues of a Cry1Ac-susceptible (DBM1Ac-S) and four Cry1Ac-resistant strains. The PxGLD protein levels detected by western blot (upper row) and quantitation of band intensity by densitometry (graph) are displayed. (C and D) Effects of Cry1Ac exposure (C) and gene silencing on *PxGLD* expression (D) in the midgut of Cry1Ac-susceptible DBM1Ac-S larvae. Two different concentrations of Cry1Ac protoxin (LC_{50}, 1 mg/L; LC_{90}, 2 mg/L) were used in the toxin exposure assays. (E) Influence of *PxGLD* gene knockdown on larval mortality in the susceptible DBM1Ac-S strain. The housekeeping gene *RPL32* was employed as the internal reference gene, and the transcript levels in the DBM1Ac-S (A), untreated (C), and buffer-treated (D and E) assays were set to 1. (F) Linkage of reduced *PxGLD* expression with the Cry1Ac resistance phenotype. Backcrossed families a and b were produced by backcrossing F1 females and males with males and females from the resistant parental NIL-R strain. The relative transcript levels for the F1, Cry1Ac-treated, and non-treated families were quantitated and normalized to the transcript level of the Cry1Ac-susceptible DBM1Ac-S larvae. The *PxGLD* and *RPL32* genes were amplified and displayed above each graph. Bars are mean ± SEM (A–E). ns, not significant; *$p < 0.05$, **$p < 0.01$, ***$p < 0.001$; one-way ANOVA adjusted by Tukey's test.

species (Figure S4B). Spatiotemporal gene expression analysis indicated that *PxGLD* is preferentially enriched in the midgut and larval stage (Figures S4C and S4D). Moreover, the transcript and protein levels of *PxGLD* were substantially decreased in the resistant larval midgut tissues compared with the susceptible counterparts (Figures 3A and 3B). Next, we treated the susceptible DBM1Ac-S larvae with 1 mg/L (LC_{50}) or 2 mg/L (LC_{90}) of Cry1Ac protoxin and measured *PxGLD* expression changes in midgut samples from the survivors. The results showed that the transcript levels of *PxGLD* were significantly lower in the Cry1Ac-treated groups than in the untreated group (Figure 3C).

To determine whether decreased expression of the *PxGLD* gene was related to Cry1Ac susceptibility, we utilized siRNA-mediated RNAi to silence its expression in the susceptible strain. RT-qPCR analysis confirmed that *PxGLD* expression was reduced in the siPxGLD-treated group compared with the buffer- and siNC-treated groups (Figure 3D). Toxicity bioassays conducted at 72 h post-injection showed that knockdown of *PxGLD* expression decreased Cry1Ac susceptibility at both 1 mg/L (LC_{50}) and 2 mg/L (LC_{90}) (Figure 3E). A genetic association test was performed to check the cosegregation of reduced expression of *PxGLD* with Cry1Ac resistance in the NIL-R strain (Figure 3F). The transcript level of *PxGLD* showed two different groups in both Cry1Ac-untreated F2 backcross families. One group displayed decreased *PxGLD* expression, while the other group showed a similar expression to the parental susceptible DBM1Ac-S strain or the F1 progeny. In addition, the ratio between the groups in the two backcross families was 1:1, which fits the theoretical inheritance ratio ($p = 1.0$; χ^2 test). However, the transcript level of *PxGLD* was reduced in all survivors from Cry1Ac-treated F2 families compared with the parental susceptible DBM1Ac-S strain or the F1 progeny, indicating that reduced *PxGLD* expression is tightly linked (cosegregated) to Cry1Ac resistance.

Reduced PxGLD decreases 20E degradation to increase 20E titer

The glucose dehydrogenase (GLD) gene encodes a flavin adenine dinucleotide (FAD)-binding flavoprotein belonging to the glucose-methanol-choline (GMC) oxidoreductase family.[38] Previous studies have found that ecdysone oxidase (EO), which mediates ecdysone degradation, belongs to the same GMC family,[38] we therefore speculated that the newly identified PxGLD might also be involved in an ecdysone degradation pathway. Sequence alignment analysis demonstrated that the PxGLD and EO proteins from different insect species (including *P. xylostella*) share four conserved FAD-binding domains, one flavin attachment loop domain, and one catalytic active site (Figure S5). We found that *PxGLD* expression and 20E titer displayed an opposing trend during the normal feeding stage of *P. xylostella* (Figure 4A), suggesting a possible relationship between the two. To investigate this further, we treated susceptible DBM1Ac-S larvae with exogenous 20E and then measured *PxGLD* expression levels. RT-qPCR results at 48 h after 20E treatment revealed that *PxGLD* expression was significantly increased compared with the control (Figure 4B). Moreover, the 20E titer was significantly increased at 48 h after knocking down *PxGLD* in the susceptible DBM1Ac-S strain (Figure 4C).

On this basis, we considered that PxGLD might participate in the metabolism of E and 20E. To test this, PxGLD was ectopically expressed in *Spodoptera frugiperda* (Sf9) cells for *in vitro* detection of enzyme activity (Figures S6A and S6B). Ultraperformance liquid chromatography-tandem mass spectrometry (UPLC-MS/MS) was employed to detect E, 20E, 3-dehydroecdysone (3DE), and 3-dehydro-20-hydroxyecdysone (3D20E), cyasterone was used as an internal UPLC control (Figures 4D and 4E). The UPLC-MS/MS analysis indicated that the recombinant PxGLD enzyme could metabolize E into 3DE (Figures 4F, 4G, 4J, 4K, and 4N) and 20E into 3D20E (Figures 4H, 4I, 4L, 4M, and 4O).

miR-8545 regulates Cry1Ac resistance via the *PxGLD*/20E module

To further ascertain how miR-8545 modulates Cry1Ac susceptibility in *P. xylostella* via the *PxGLD*/20E module, agomir-8545 was injected into early third-instar larvae from the susceptible DBM1Ac-S strain. The expression level of *PxGLD* was suppressed at 48 h post-injection (Figure 5A). Assessment of

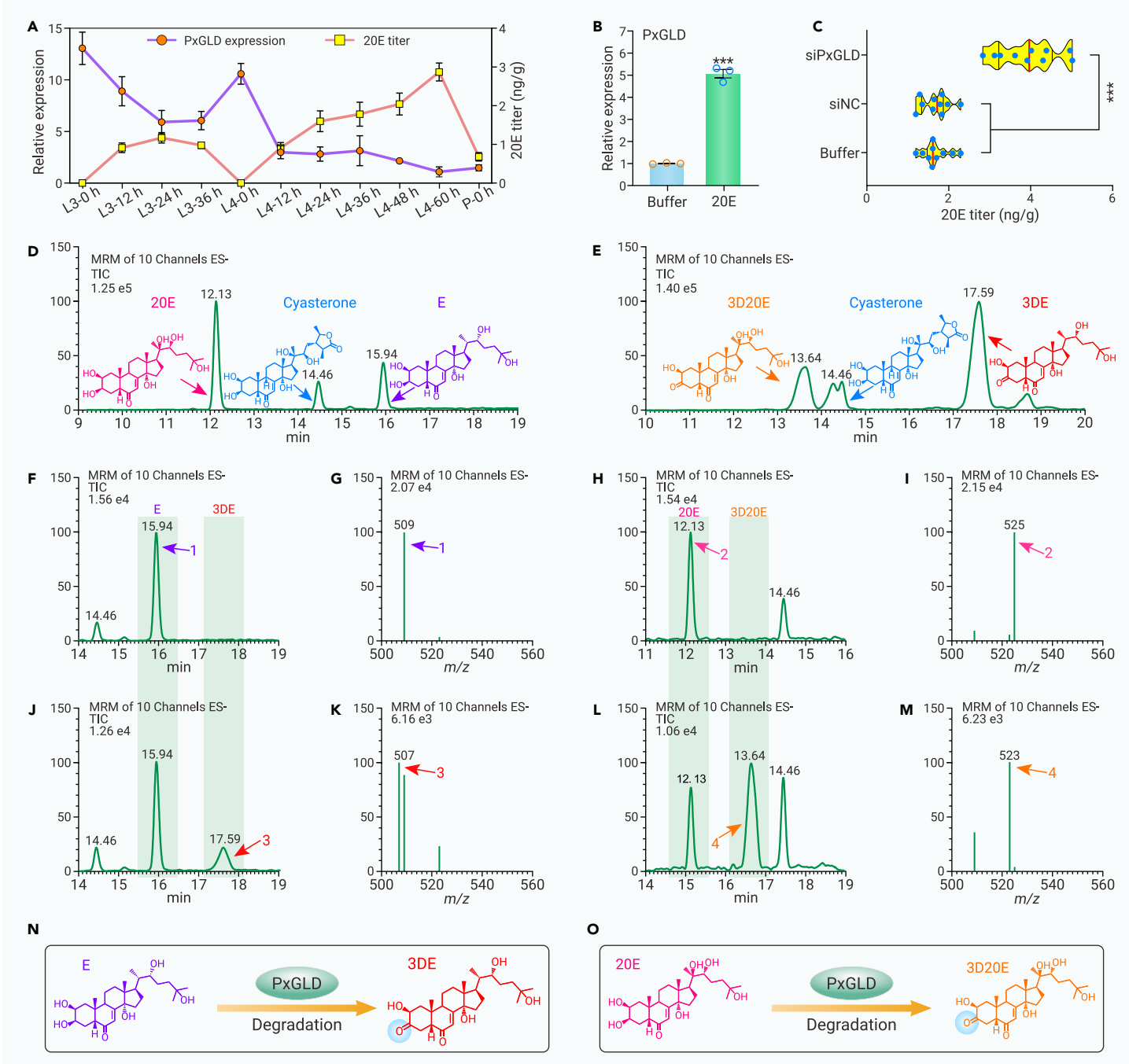

Figure 4. PxGLD is an ecdysteroid-degrading enzyme and its reduction causes an increase in 20E titer (A) The transcript levels of *PxGLD* and 20E titer changes in third-instar larvae (L3), fourth-instar larvae (L4), and pupae (P) of *P. xylostella*. (B) Effects of 20E on *PxGLD* expression in the Cry1Ac-susceptible DBM1Ac-S larvae. (C) Violin plot shows the effect of *PxGLD* silencing on 20E titer in the Cry1Ac-susceptible DBM1Ac-S larvae. Each blue dot indicates the mean 20E titer in two fourth-instar larvae after microinjection with buffer, siNC, or siPxGLD. Median and quartile values are displayed via red and black vertical lines respectively, the left and right edges of the violin plots illustrate min and max values. *RPL32* was employed as the internal reference gene, and the transcript levels of the lowest expression stage (A) and buffer-treated group (B and C) were set to 1. Bars are mean ± SEM (A–C). ns, not significant; *$p < 0.05$, **$p < 0.01$, ***$p < 0.001$; one-way ANOVA adjusted by Tukey's test. (D and E) Representative MRM chromatograms of standard samples of ecdysone (E), 20-hydroxyecdysone (20E), 3-dehydroecdysone (3DE), 3-dehydro-20-hydroxyecdysone (3D20E), and cyasterone detected by UPLC-MS/MS. (F–I) The catalytic effect of proteins from the supernatant of Sf9 (control) cells on E and 20E. 1, E + $HCOO^-$ (F and G); 2, 20E + $HCOO^-$ (H and I). (J–M) Sf9-expressed recombinant PxGLD protein catalyzes E and 20E oxidative metabolism. 3, 3DE + $HCOO^-$ (J and K); 4, 3D20E + $HCOO^-$ (L and M). (N and O) Schematic diagram of the metabolism processes of E and 20E by Sf9-expressed recombinant PxGLD protein. E and 20E can be respectively degraded into 3DE (N) and 3D20E (O).

protein levels confirmed that PxGLD was also reduced (Figure 5B). Meanwhile, 20E titer was found to be significantly increased (Figure 5C). Toxicity bioassays conducted at 72 h post-injection showed a decrease in Cry1Ac susceptibility at 2 mg/L (LC_{90}) in the agomir-8545-injected group (Figure 5D). In contrast, the transcript and protein levels of *PxGLD* were elevated (Figures 5E and 5F) and the 20E titer reduced (Figure 5G) 48 h post-injection of antagomir-8545 in the Cry1Ac-resistant NIL-R strain, and the larval mortality to Cry1Ac protoxin at 1,000 mg/L (LC_{10}) increased in this group (Figure 5H).

The approach of specifically disrupting the binding of miRNA to mRNA target sites by injecting gene-specific target protectors *in vivo* was used to confirm the direct regulation of *PxGLD* by miR-8545 (Figure 5I). Administration of the miR-8545 target protector against *PxGLD* increased both transcript and protein levels of *PxGLD* (Figures 5J and 5K), and a subsequent bioassay showed that larval mortality to Cry1Ac protoxin at 1,000 mg/mL (LC_{10}) was increased (Figure 5L). These results show that miR-8545 mediates Cry1Ac tolerance/resistance via the *PxGLD*/20E module.

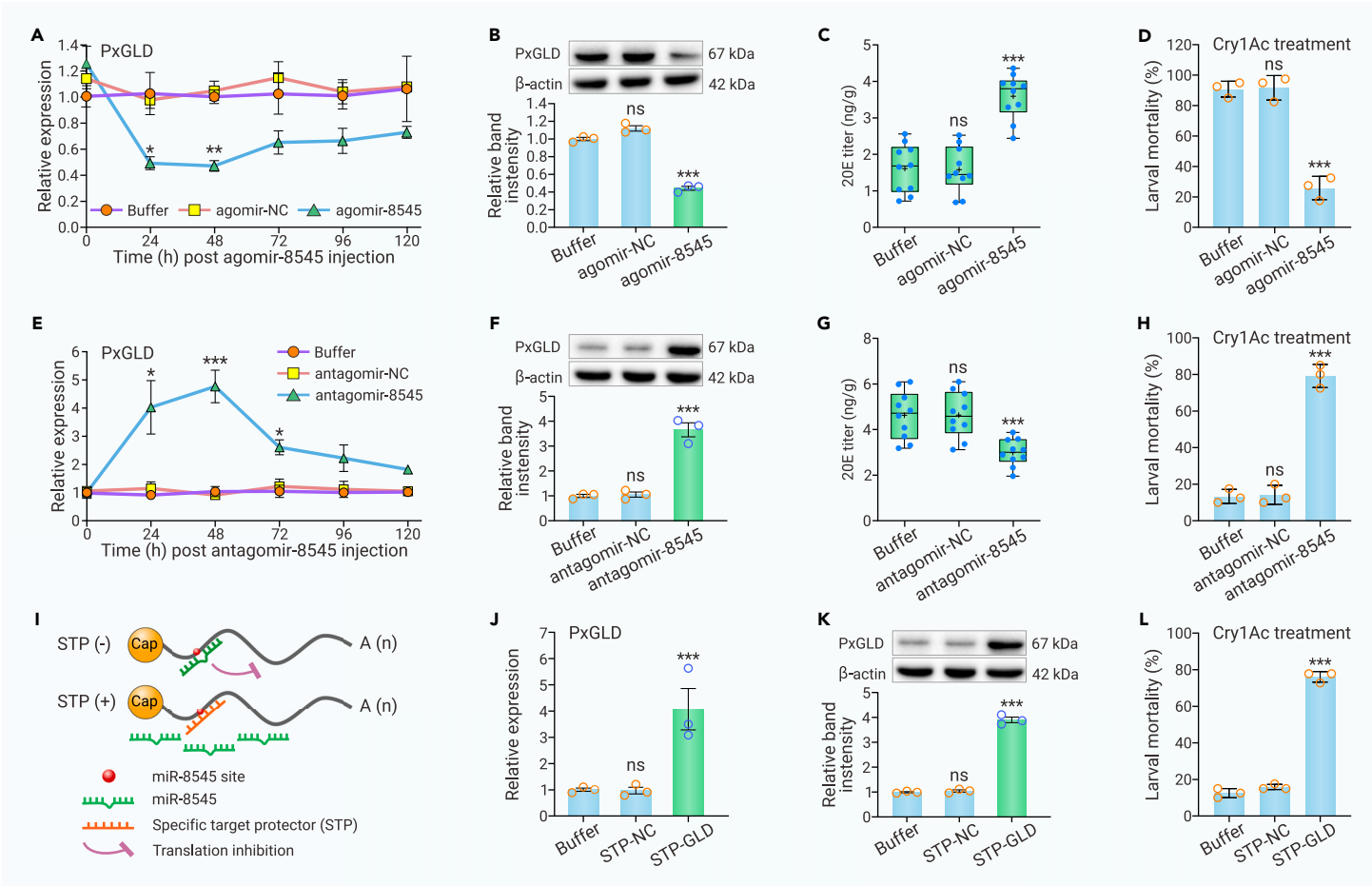

Figure 5. miR-8545 mediates Cry1Ac resistance in *P. xylostella* through modulating *PxGLD* expression (A) Effect of agomir-8545 microinjection on *PxGLD* transcript levels at various time points in the Cry1Ac-susceptible DBM1Ac-S larvae. (B–D) Effect of agomir-8545 microinjection for 48 h on the *PxGLD* protein levels (B), 20E titer (C), and larval mortality (D) in the Cry1Ac-susceptible DBM1Ac-S larvae. (E) Effect of antagomir-8545 microinjection on the *PxGLD* transcript levels at various time points in the Cry1Ac-resistant NIL-R larvae. (F–H) Effect of antagomir-8545 microinjection for 48 h on *PxGLD* protein levels (F), 20E titer (G), and larval mortality (H) in the Cry1Ac-resistant NIL-R larvae. (I) Schematic diagram of the principle of gene-specific target protector (STP). The STP can specifically target the binding region of miRNA on the target gene, which prevents any interaction between them. (J–L) Effect of STP-GLD microinjection for 48 h on the transcript (J) and protein (K) levels of *PxGLD* and on larval mortality (L) in the resistant NIL-R strain. *RPL32* was employed as the internal reference gene, and the transcript levels in the buffer-treated samples (A, E, and J) were set to 1. Bars are mean ± SEM (A–H and J–L). ns, not significant; *$p < 0.05$, **$p < 0.01$, ***$p < 0.001$; one-way ANOVA adjusted by Tukey's test.

A miR-8545 knockout reduces Cry1Ac resistance

To establish a homozygous miR-8545 knockout (miR-8545KO) in the NIL-R strain, a miR-8545-specific sgRNA was employed (Figure S7A), resulting in a 7-bp deletion (Figures S7B and S7C). Homozygous individuals were sib-crossed to construct a stable homozygous mutant strain (Figure S7D) and RT-PCR was used to confirm that miR-8545 had successfully been knocked out (Figure S7E). The transcript (Figure 6A) and protein (Figure 6B) levels of *PxGLD* were both found to have increased in the miR-8545KO strain, while 20E titer was significantly decreased (Figure 6C). RT-qPCR showed that the transcript level of *PxMAP4K4* was reduced in this strain while the expression levels of midgut genes related to Cry1Ac resistance increased (Figure 6D). Bioassay results demonstrated a significant rise in sensitivity to Cry1Ac, with the LC_{50} value decreasing from 4,040 to 27 mg/L (Figure 6E). In addition, we observed that both gut weight (Figures 6F and 6G) and pupae size (Figure 6H) in the miR-8545KO strain had increased. Such a difference in size was observed previously when an imbalance between JH and 20E occurred,[6] in particular a larger pupal size was observed when the balance shifted toward JH, which would parallel the situation here in which 20E titer is reduced in miR-8545KO.

Reduced PxDfd binding results in miR-8545 overexpression

To further analyze the transcriptional regulatory mechanisms responsible for the overexpression of miR-8545 in the Cry1Ac-resistant strain, the promoter sequences of miR-8545 were cloned from both Cry1Ac-susceptible DBM1Ac-S and Cry1Ac-resistant NIL-R strains. Sequence comparison results indicated that there were no potential *cis*-mutations in the promoters of miR-8545 that could account for the differential expression (Figure S8). Accordingly, we considered whether transcription factor (TF)-mediated *trans*-regulation might play a key role in regulating the transcription of miR-8545. To test this hypothesis, the JASPAR and PROMO databases were used to predict candidate TFs. Among the candidates, two homeodomain-containing TFs—deformed (PxDfd) and Fushi tarazu (PxFtz) —were predicted to bind to the miR-8545 promoter (Figure 7A).

To explore whether PxDfd and PxFtz could modulate the transcription of miR-8545, a construct containing the promoter of miR-8545 fused to a luciferase reporter was introduced into *Drosophila* S2 cells alongside expression constructs for each TF. Results showed that PxDfd, but not PxFtz, affected (inhibited) the transcriptional activity of miR-8545 (Figure 7B). Three potential PxDfd binding sites (DBSs) within the miR-8545 promoter were predicted by bioinformatic analyses—all upstream of the transcription start site (Figure S8). To identify the functional DBS (s), we used various truncated promoter fragments fused to luciferase. This indicated that the most upstream of the three sites (DSB1) was the functional one (Figure 7C). An electrophoretic mobility shift assay (EMSA) and a yeast one-hybrid (Y1H) assay were employed to confirm that PxDfd directly binds to the DBS1 motif. In the EMSA assay, PxDfd was found to specifically bind to the DBS1 probe (Figure 7D). No significant band shift was observed in the absence of PxDfd or when PxDfd was incubated with a mutated probe (Figure 7D). In the Y1H assay, only yeast strains co-transformed with PxDfd and the DBS1 motif grew normally in the selective medium (Figure 7E). These results indicated that PxDfd inhibits the transcription of miR-8545 via binding to the DBS1 motif.

A phylogenetic analysis showed that the cloned PxDfd is evolutionarily conserved and clusters with the Lepidoptera insect group (Figures S9A–S9C). The spatiotemporal transcription profile of *PxDfd* was determined and revealed

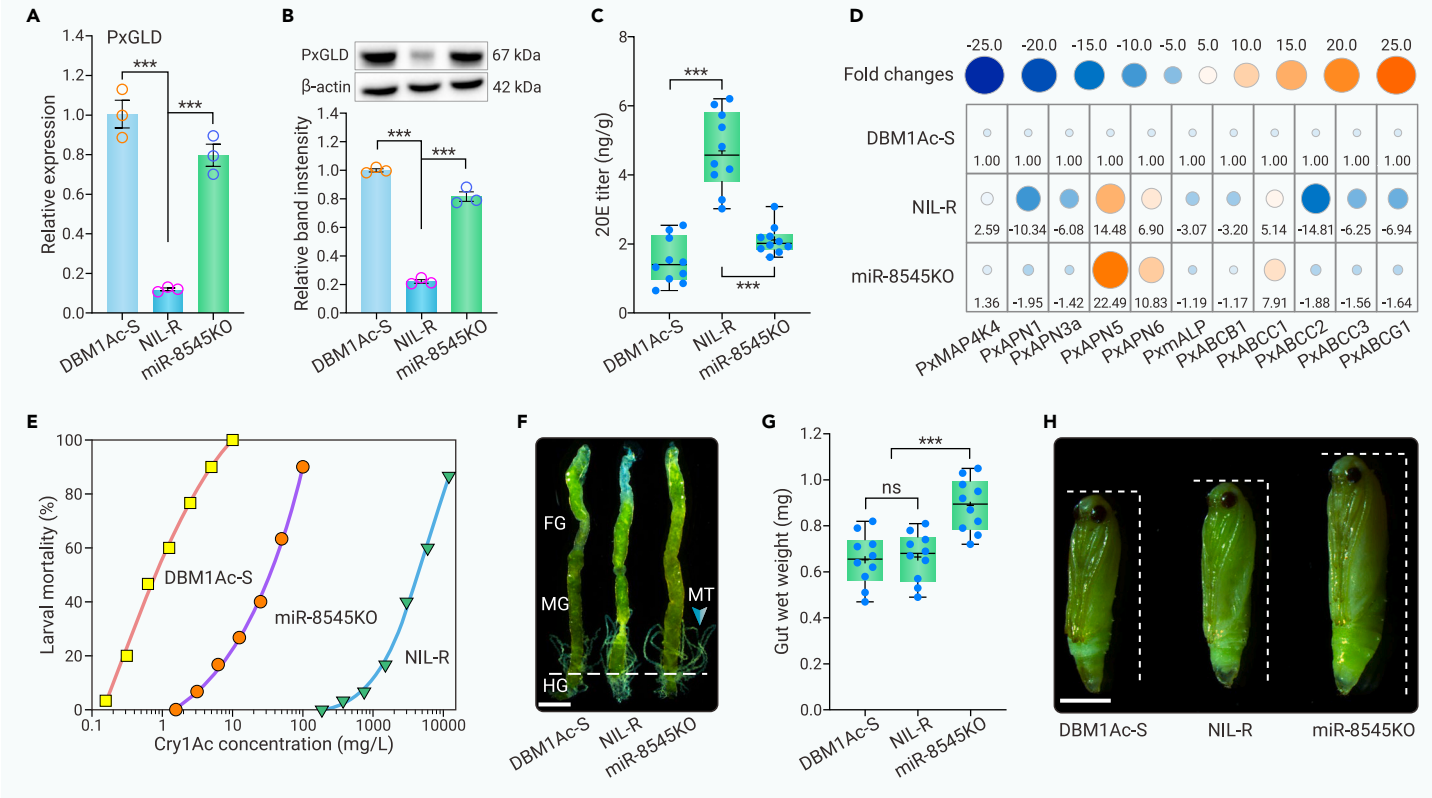

Figure 6. CRISPR-Cas9-mediated knockout of miR-8545 increases Cry1Ac sensitivity of *P. xylostella* (A–C) Impact of miR-8545 knockout on the transcript (A) and protein (B) levels of *PxGLD*, and on 20E titer (C). (D) The expression levels of *PxMAP4K4* and various midgut genes in the miR-8545 knockout strain miR-8545KO. *RPL32* was employed as the internal reference gene, and the transcript level in the DBM1Ac-S larvae (A and D) was set to 1. The expression levels for different genes are indicated by spheres of distinct sizes and colors, and by the values displayed. (E–H) Effect of miR-8545 knockout on larval mortality (E), midgut weight (F and G), and pupal size (H). Scale bar, 5 μm. Bars are mean ± SEM (A–C and G). ns, not significant; *$p < 0.05$, **$p < 0.01$, ***$p < 0.001$; one-way ANOVA adjusted by Tukey's test.

that *PxDfd* was enriched in the head, egg, and first-instar larvae (Figures S9D and S9E). To assess whether *PxDfd* might be associated with Cry1Ac resistance, the transcript levels of *PxDfd* were monitored in the midgut tissues of various Cry1Ac-susceptible and Cry1Ac-resistant strains. The data showed that the midgut levels of *PxDfd* transcripts were reduced in all resistant strains (Figure 7F). The functional role of *PxDfd* in regulating expression of miR-8545 *in vivo* was further demonstrated by RNAi. Silencing of *PxDfd* in susceptible DBM1Ac-S larvae was accompanied by an increased expression of both miR-8545 precursor (Pre-miR-8545) and mature miR-8545 (Figure 7G). In addition, this silencing of *PxDfd* increased the transcript level of *PxMAP4K4* and reduced the relative expression levels of midgut receptor and non-receptor genes (Figure 7G). Toxicity bioassays conducted at 72 h post-microinjection showed that knockdown of *PxDfd* expression decreased larval mortality to Cry1Ac protoxin at 2 mg/L (LC_{90}) (Figure 7H).

A putative negative feedback loop decreases 20E overproduction

Subsequently, we decided to investigate whether 20E can induce PxDfd-mediated changes in the miR-8545/*PxGLD* module during the feeding stage of *P. xylostella*. Susceptible DBM1Ac-S larvae were treated with exogenous 20E and their weights were measured 48 h post-treatment. The weight of the surviving larvae indicated two distinct clusters: robust (larvae did not exhibit significant growth and developmental inhibition or deformity) and weak (larvae exhibited significant growth and developmental inhibition and deformity). In the buffer-treated groups, only a small minority (4.2%) showed the weak phenotype compared with 72.0% for the 20E-treated larvae (Figure 8A). Subsequently, RT-qPCR showed a substantial increase in expression levels of both *PxDfd* (Figure 8B) and *PxGLD* (Figure 8D), and a significant reduction in transcript levels of miR-8545 (Figure 8C) in the 20E-treated group compared with the buffer-treated group. There were no significant differences in the expression of these genes between the weak and robust larvae of the buffer-treated strain, suggesting that the small percentage of weak larvae may not be related to the PxDfd/miR-8545/*PxGLD* axis. In contrast, in the 20E-treated group, the expression changes were more significant in the robust larvae than in the weak larvae, indicating that those larvae that dealt better with the excess 20E showed improved growth characteristics. To further decode the interplay between 20E exposure and the PxDfd/miR-8545/*PxGLD* axis, we investigated the effect of 20E treatment on *PxDfd*-silenced DBM1Ac-S larvae. The results demonstrated that 20E partially decreases miR-8545 expression (Figure 8E) and increases *PxGLD* expression (Figure 8F) in the *PxDfd*-silenced individuals. These results suggest that excess 20E can suppress the PxDfd/miR-8545/*PxGLD* regulatory axis through a negative feedback mechanism (Figure 8G).

DISCUSSION

Many pathogens, such as bacteria, viruses, and fungi, can cause disease in their animal or insect hosts.[39] Consequently, the host needs to have a rapid and robust defense response to repel pathogen infection. We have previously described a Bt resistance phenotype in *P. xylostella*, in which expression of multiple receptors for the primary Bt virulence factors (Cry toxins) are downregulated.[24,40] To mitigate the physiological costs of this downregulation, non-receptor paralogs are upregulated, allowing the insect to maintain fitness while defending against the pathogen. The expression of these midgut proteins was found to be controlled by a MAPK signaling pathway, which was constitutively activated in strains that had evolved high level resistance to Bt.[25,29] The response was also found to be modulated by the hormones 20E and JH, with the former controlling the downregulation of the receptors, while the latter influences the expression of the paralogs.[6] A tandem increase in both hormones resulted in the balanced response observed upon exposure to Bt, or in the resistant strains, in which fitness was maintained alongside defense. 20E and JH have long been known to act in tandem to control the timing of crucial developmental processes such as molting and metamorphosis[41] and more recently in regulating some aspects of immunity.[5] Our work extends our understanding of the pleiotropic effects of this hormone pair to include a localized response within the midgut tissues of the feeding larval stage of an insect. We have recently studied the mechanism by which JH titer is increased upon exposure to a Bt toxin and found that this involves m^6A-epigenetic regulation of an esterase that can degrade JH.[30] The data presented here show that the

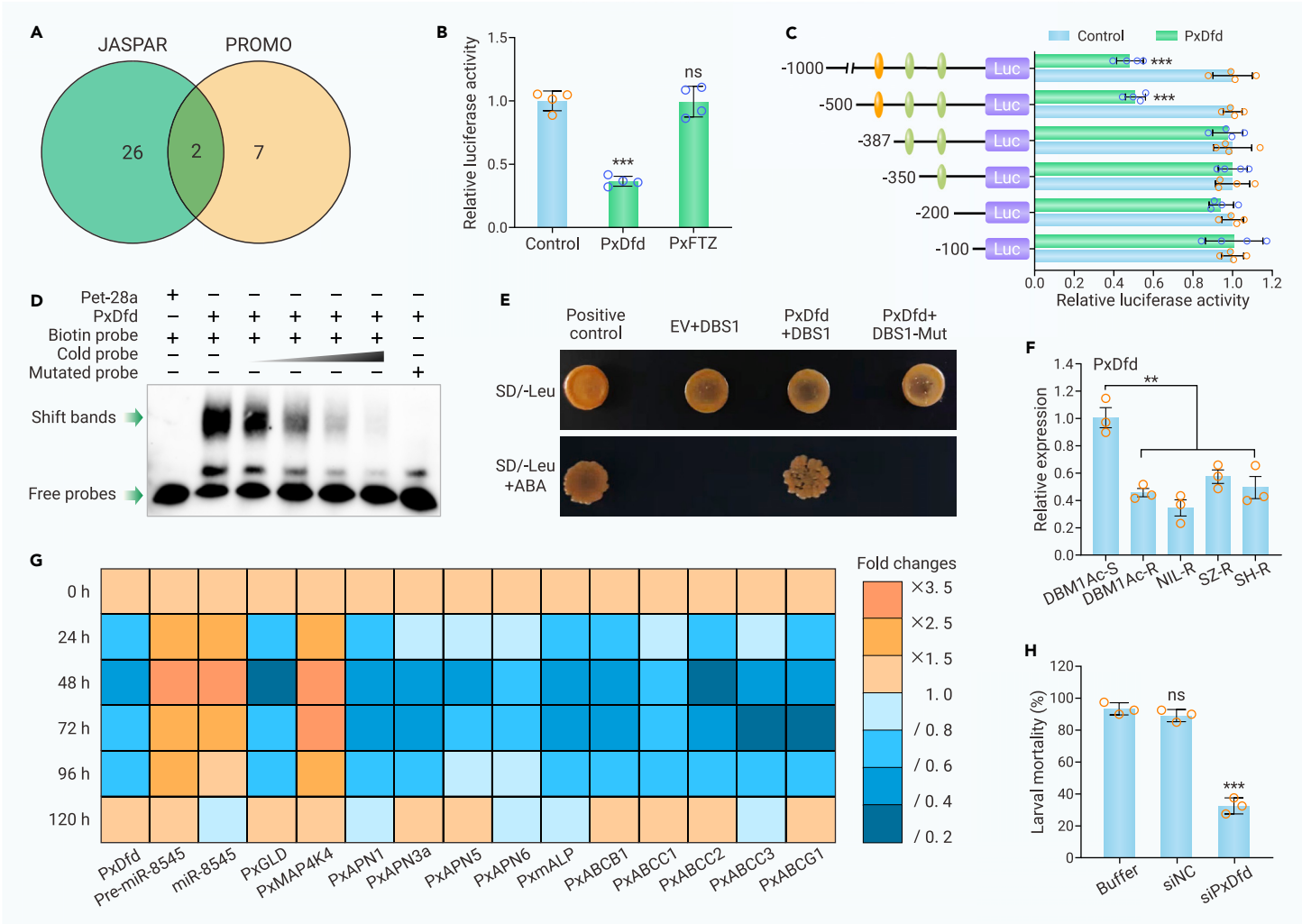

Figure 7. PxDfd represses miR-8545 promoter activity through the DBS1 motif (A) The JASPAR and PROMO databases were employed to predict potential transcription factor (TF) binding to the miR-8545 promoter region. (B) Influence of two TFs on the promoter activity of miR-8545. Each pAc5.1-TF expression vector and pGL4.10-promoter reporter plasmid were co-transfected into S2 cells. The empty pAc5.1 vector was utilized as a control. (C) Effects of PxDfd on truncated miR-8545 promoters. The empty pAc5.1 vector was utilized as a control. (D) Electrophoretic mobility shift assay (EMSA). The biotin-labeled DBS1 probe (20 fmol) and mutant probes (20 fmol), and the unlabeled competing cold probes (200, 500, 1,000, and 2,000 fmol) were used. The black triangle indicates increasing amounts of competing cold probes. (E) Yeast one-hybrid (Y1H) assay. (F) The expression of *PxDfd* was analyzed in the larval midgut tissues from the Cry1Ac-susceptible DBM1Ac-S strain and four Cry1Ac-resistant *P. xylostella* strains. (G and H) Impact of *PxDfd* silencing on the transcript level of pre-miR-8545, miR-8545, and midgut genes (G), and on larval susceptibility to 2 mg/L (LC_{90}) of Cry1Ac protoxin (H) in the susceptible DBM1Ac-S strain. *RPL32* was employed as the internal reference gene, and the transcript levels in the DBM1Ac-S (F) and untreated (G) samples were set to 1. Bars are mean ± SEM (B, C, F, and H). ns, not significant; $*p < 0.05$, $**p < 0.01$, $***p < 0.001$; one-way ANOVA adjusted by Tukey's test.

increase in 20E titer in response to Bt is due to a miRNA-mediated pathway leading to the decreased expression of a newly identified ecdysteroid-degrading glucose dehydrogenase (*PxGLD*). In general, ecdysone (E) needs to be converted into 20E to exert its physiological functions.[42] In addition, 20E needs to be degraded after completing its biological functions during the molting, metamorphosis, and reproduction stages.[38] Previous studies have reported that an EO can metabolize E to 3DE[43-45] and a cytochrome P450 gene CYP18A1 can metabolize 20E to 20-hydroxyecdysonoic acid (20Eoic).[46] The conversion of E and 20E into 3-dehydroecdysteroids (3DE and 3D20E) is a main pathway in *Drosophila melanogaster* larvae.[47] Our results showed that the Sf9-expressed PxGLD protein can metabolize both E to 3DE and 20E to 3D20E, and so introduce this enzyme as one that may also be involved in other ecdysone-mediated processes. The encoding protein was annotated as a glucose dehydrogenase on the basis of sequence analysis, but we have no evidence as to whether it has this particular activity. Exposure of *P. xylostella* to exogenous 20E resulted in significant growth defects and also resulted in the elevation of levels of PxGLD. This is consistent with the possibility that the enzyme participates in a negative feedback loop (via miR-8545 and PxDfd in this case) to control 20E titer in both this and potentially other 20E-mediated processes.

Although there is a coordinated increase in both 20E and JH in response to Bt intoxication, we have identified different pathways controlling the titers of these two hormones. It is still unclear what the initial signal for the response is, perhaps binding of the toxin to the receptor, or the formation of the toxin pore, and it is also unknown in what way this signal is transmitted to the hormone titer regulation pathway. We have shown that this pathway is constitutively altered in the resistant strain and have previously demonstrated that the resistance phenotype in that strain is the result of a transposon insertion into the promoter region of the *MAP4K4* gene.[29] How that MAPK signaling pathway feeds back to this miRNA pathway is also unclear, as is the full extent to which the toxin-induced response and the evolved resistance phenotype are linked. Although we better understand how insect pests such as *P. xylostella* control their response to pathogens such as Bt, it opens up potential new approaches for their control such as novel RNAi targets.[48]

MATERIALS AND METHODS

See supplemental information for details.

DATA AND CODE AVAILABILITY

The full-length cDNA sequences of all the cloned genes in this study have been deposited in the GenBank database (accession nos. OR130726–OR130730). The authors declare that the data supporting the findings of this study are available within the paper and its supplemental materials.

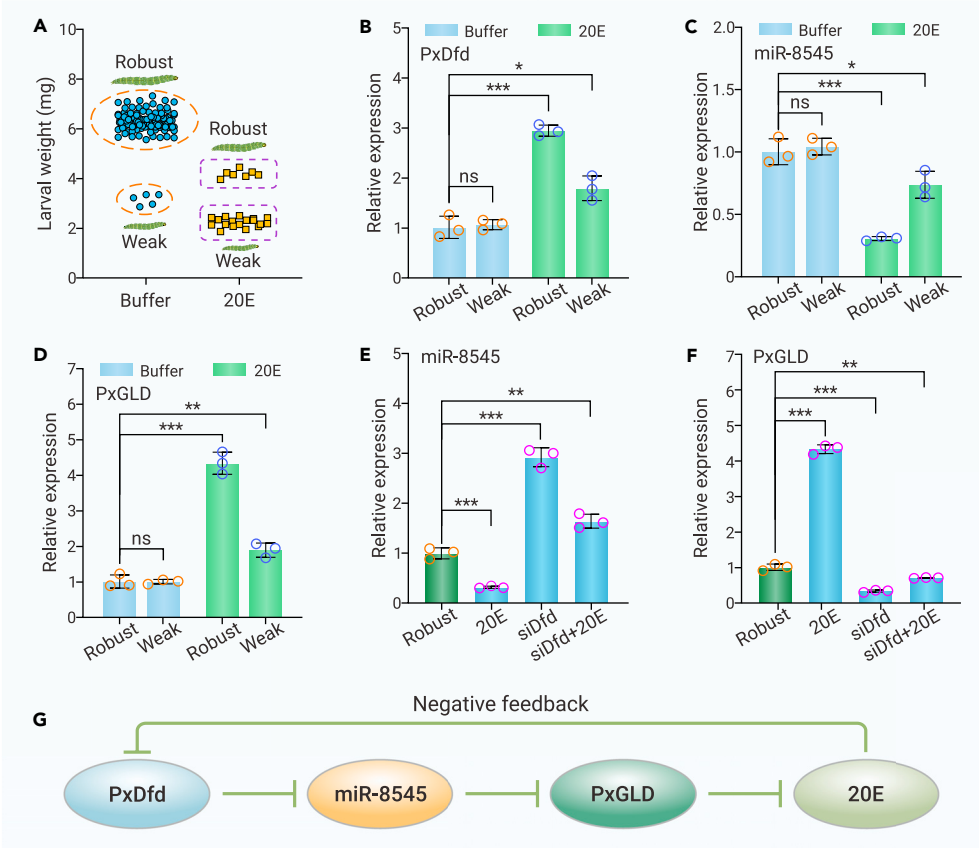

Figure 8. 20E regulates the PxDfd/miR-8545/*PxGLD* axis via negative feedback (A) Effect of exogenous 20E treatment on larval weight in the Cry1Ac-susceptible DBM1Ac-S strain. (B–D) Influence of exogenous 20E treatment on the transcript levels of *PxDfd* (B), miR-8545 (C), and *PxGLD* (D) in robust and weak DBM1Ac-S larvae. (E and F) Impact of exogenous 20E treatment on the transcript levels of miR-8545 (E) and *PxGLD* (F) in the *PxDfd*-silenced DBM1Ac-S individuals. (G) Schematic diagram of the 20E-regulated PxDfd/miR-8545/*PxGLD* axis through the negative feedback mechanism. *RPL32* (B, D, and F) and *U6* (C and E) were employed as the respective internal reference genes, and the transcript levels in the buffer-treated robust larvae were set to 1. Bars are mean ± SEM (B–F). ns, not significant; $*p < 0.05$, $**p < 0.01$, $***p < 0.001$; one-way ANOVA adjusted by Tukey's test.

REFERENCES

1. Roy, S., Saha, T.T., Zou, Z., et al. (2018). Regulatory pathways controlling female insect reproduction. Annu. Rev. Entomol. ***63***: 489–511. https://doi.org/10.1146/annurev-ento-020117-043258.
2. Truman, J.W., and Riddiford, L.M. (2019). The evolution of insect metamorphosis: a developmental and endocrine view. Phil. Trans. R. Soc. B. ***374***(1783): 20190070. https://doi.org/10.1098/rstb.2019.0070.
3. Bellés, X. (2020). Insect Metamorphosis: From Natural History to Regulation of Development and Evolution (London: Academic Press).
4. Ji, X., Wang, L., Li, X., et al. (2024). Hormonal control of *fruitless* expression and male sexual orientation in *Drosophila*. Innov. Life ***2***(1): 100060. https://doi.org/10.59717/j.xinn-life.2024.100060.
5. Nunes, C., Sucena, É., and Koyama, T. (2021). Endocrine regulation of immunity in insects. FEBS J. ***288***(13): 3928–3947. https://doi.org/10.1111/febs.15581.
6. Guo, Z., Kang, S., Sun, D., et al. (2020). MAPK-dependent hormonal signaling plasticity contributes to overcoming *Bacillus thuringiensis* toxin action in an insect host. Nat. Commun. ***11***(1): 3003. https://doi.org/10.1038/s41467-020-16608-8.
7. Nielsen-LeRoux, C., Gaudriault, S., Ramarao, N., et al. (2012). How the insect pathogen bacteria *Bacillus thuringiensis* and *Xenorhabdus/Photorhabdus* occupy their hosts. Curr. Opin. Microbiol. ***15***(3): 220–231. https://doi.org/10.1016/j.mib.2012.04.006.
8. Pardo-López, L., Soberón, M., and Bravo, A. (2013). *Bacillus thuringiensis* insecticidal three-domain Cry toxins: mode of action, insect resistance and consequences for crop protection. FEMS Microbiol. Rev. ***37***(1): 3–22. https://doi.org/10.1111/j.1574-6976.2012.00341.x.
9. Raymond, B., Johnston, P.R., Nielsen-LeRoux, C., et al. (2010). *Bacillus thuringiensis*: an impotent pathogen? Trends Microbiol. ***18***(5): 189–194. https://doi.org/10.1016/j.tim.2010.02.006.
10. Jurat-Fuentes, J.L., Heckel, D.G., and Ferré, J. (2021). Mechanisms of resistance to insecticidal proteins from *Bacillus thuringiensis*. Annu. Rev. Entomol. ***66***: 121–140. https://doi.org/10.1146/annurev-ento-052620-073348.
11. Pinos, D., Andrés-Garrido, A., Ferré, J., et al. (2021). Response mechanisms of invertebrates to *Bacillus thuringiensis* and its pesticidal proteins. Microbiol. Mol. Biol. Rev. ***85***(1): e00007-20. https://doi.org/10.1128/MMBR.00007-20.
12. Bravo, A., Pacheco, S., Gómez, I., et al. (2023). Mode of action of *Bacillus thuringiensis* Cry pesticidal proteins. Adv. Insect Physiol ***65***: 55–92. https://doi.org/10.1016/bs.aiip.2023.09.003.
13. Fabrick, J.A., and Wu, Y. (2023). Mechanisms and molecular genetics of insect resistance to insecticidal proteins from *Bacillus thuringiensis*. Adv. Insect Physiol ***65***: 123–183. https://doi.org/10.1016/bs.aiip.2023.09.005.
14. Bravo, A., Likitvivatanavong, S., Gill, S.S., et al. (2011). *Bacillus thuringiensis*: a story of a successful bioinsecticide. Insect Biochem. Mol. Biol. ***41***(7): 423–431. https://doi.org/10.1016/j.ibmb.2011.02.006.
15. Carrière, Y., Crickmore, N., and Tabashnik, B.E. (2015). Optimizing pyramided transgenic Bt crops for sustainable pest management. Nat. Biotechnol. ***33***(2): 161–168. https://doi.org/10.1038/nbt.3099.
16. Tabashnik, B.E., Liesner, L.R., Ellsworth, P.C., et al. (2021). Transgenic cotton and sterile insect releases synergize eradication of pink bollworm a century after it invaded the United States. Proc. Natl. Acad. Sci. USA ***118***: e2019115118. https://doi.org/10.1073/pnas.2019115118.
17. Jin, M., North, H.L., Peng, Y., et al. (2023). Adaptive evolution to the natural and anthropogenic environment in a global invasive crop pest, the cotton bollworm. Innovation ***4***(4): 100454. https://doi.org/10.1016/j.xinn.2023.100454.
18. Badran, A.H., Guzov, V.M., Huai, Q., et al. (2016). Continuous evolution of *Bacillus thuringiensis* toxins overcomes insect resistance. Nature ***533***(7601): 58–63. https://doi.org/10.1038/nature17938.
19. Tabashnik, B.E., and Carrière, Y. (2017). Surge in insect resistance to transgenic crops and prospects for sustainability. Nat. Biotechnol. ***35***(10): 926–935. https://doi.org/10.1038/nbt.3974.
20. Gould, F., Brown, Z.S., and Kuzma, J. (2018). Wicked evolution: Can we address the sociobiological dilemma of pesticide resistance? Science ***360***(6390): 728–732. https://doi.org/10.1126/science.aar3780.
21. Tabashnik, B.E., Fabrick, J.A., and Carrière, Y. (2023). Global patterns of insect resistance to transgenic Bt crops: the first 25 years. J. Econ. Entomol. ***116***: 297–309. https://doi.org/10.1093/jee/toac183.
22. Furlong, M.J., Wright, D.J., and Dosdall, L.M. (2013). Diamondback moth ecology and management: problems, progress, and prospects. Annu. Rev. Entomol. ***58***: 517–541. https://doi.org/10.1146/annurev-ento-120811-153605.
23. Crickmore, N. (2016). *Bacillus thuringiensis* resistance in *Plutella*—too many trees? Curr. Opin. Insect Sci. ***15***: 84–88. https://doi.org/10.1016/j.cois.2016.04.007.
24. Guo, Z., Kang, S., Chen, D., et al. (2015). MAPK signaling pathway alters expression of midgut ALP and ABCC genes and causes resistance to *Bacillus thuringiensis* Cry1Ac toxin in diamondback moth. PLoS Genet. ***11***(4): e1005124. https://doi.org/10.1371/journal.pgen.1005124.
25. Guo, Z., Kang, S., Wu, Q., et al. (2021). The regulation landscape of MAPK signaling cascade for thwarting *Bacillus thuringiensis* infection in an insect host. PLoS Pathog. ***17***(9): e1009917. https://doi.org/10.1371/journal.ppat.1009917.
26. Guo, L., Cheng, Z., Qin, J., et al. (2022). MAPK-mediated transcription factor GATAd contributes to Cry1Ac resistance in diamondback moth by reducing *PxmALP* expression. PLoS Genet. ***18***(2): e1010037. https://doi.org/10.1371/journal.pgen.1010037.
27. Sun, D., Zhu, L., Guo, L., et al. (2022). A versatile contribution of both aminopeptidases N and ABC transporters to Bt Cry1Ac toxicity in the diamondback moth. BMC Biol. ***20***(1): 33. https://doi.org/10.1186/s12915-022-01226-1.
28. Guo, Z., Guo, L., Qin, J., et al. (2022). A single transcription factor facilitates an insect host combating *Bacillus thuringiensis* infection while maintaining fitness. Nat. Commun. ***13***(1): 6024. https://doi.org/10.1038/s41467-022-33706-x.

29. Guo, Z., Guo, L., Bai, Y., et al. (2023). Retrotransposon-mediated evolutionary rewiring of a pathogen response orchestrates a resistance phenotype in an insect host. Proc. Natl. Acad. Sci. USA ***120***(14): e2300439120. https://doi.org/10.1073/pnas.2300439120.
30. Guo, Z., Bai, Y., Zhang, X., et al. (2024). RNA m^6A methylation suppresses insect juvenile hormone degradation to minimize fitness costs in response to a pathogenic attack. Adv. Sci. ***11***(6): e2307650. https://doi.org/10.1002/advs.202307650.
31. Zhou, J., Guo, Z., Kang, S., et al. (2020). Reduced expression of the P-glycoprotein gene *PxABCB1* is linked to resistance to *Bacillus thuringiensis* Cry1Ac toxin in *Plutella xylostella* (L.). Pest Manag. Sci. ***76***(2): 712–720. https://doi.org/10.1002/ps.5569.
32. Guo, Z., Sun, D., Kang, S., et al. (2019). CRISPR/Cas9-mediated knockout of both the *PxABCC2* and *PxABCC3* genes confers high-level resistance to *Bacillus thuringiensis* Cry1Ac toxin in the diamondback moth, *Plutella xylostella* (L.). Insect Biochem. Mol. Biol. ***107***: 31–38. https://doi.org/10.1016/j.ibmb.2019.01.009.
33. Ouyang, C.Z., Ye, F., Wu, Q.J., et al. (2023). CRISPR/Cas9-based functional characterization of *PxABCB1* reveals its roles in the resistance of *Plutella xylostella* (L.) to Cry1Ac, abamectin and emamectin benzoate. J. Integr. Agric. ***22***(10): 3090–3102. https://doi.org/10.1016/j.jia.2023.05.023.
34. Sun, D., Xu, Q., Guo, L., et al. (2024). The role of GPI-anchored membrane-bound alkaline phosphatase in the mode of action of Bt Cry1A toxins in the diamondback moth. Fundam. Res. https://doi.org/10.1016/j.fmre.2024.05.007.
35. Mi, S., Cai, T., Hu, Y., et al. (2008). Sorting of small RNAs into *Arabidopsis* argonaute complexes is directed by the 5′ terminal nucleotide. Cell ***133***(1): 116–127. https://doi.org/10.1016/j.cell.2008.02.034.
36. Xie, W., Lei, Y., Fu, W., et al. (2012). Tissue-specific transcriptome profiling of *Plutella xylostella* third instar larval midgut. Int. J. Biol. Sci. ***8***(8): 1142–1155. https://doi.org/10.7150/ijbs.4588.
37. Guo, X., Ma, Z., Du, B., et al. (2018). Dop1 enhances conspecific olfactory attraction by inhibiting miR-9a maturation in locusts. Nat. Commun. ***9***(1): 1193. https://doi.org/10.1038/s41467-018-03437-z.
38. Iga, M., and Kataoka, H. (2012). Recent studies on insect hormone metabolic pathways mediated by cytochrome P450 enzymes. Biol. Pharm. Bull. ***35***(6): 838–843. https://doi.org/10.1248/bpb.35.838.
39. Lai, Y., Zheng, W., Zheng, Y., et al. (2024). Unveiling a novel entry gate: Insect foregut as an alternative infection route for fungal entomopathogens. Innovation ***5***(4): 100644. https://doi.org/10.1016/j.xinn.2024.100644.
40. Qin, J., Guo, L., Ye, F., et al. (2021). MAPK-activated transcription factor PxJun suppresses *PxABCB1* expression and confers resistance to *Bacillus thuringiensis* Cry1Ac toxin in *Plutella xylostella* (L.). Appl. Environ. Microbiol. ***87***(13): e00466-21. https://doi.org/10.1128/AEM.00466-21.
41. Dubrovsky, E.B. (2005). Hormonal cross talk in insect development. Trends Endocrinol. Metab. ***16***(1): 6–11. https://doi.org/10.1016/j.tem.2004.11.003.
42. Yamanaka, N., Rewitz, K.F., and O'Connor, M.B. (2013). Ecdysone control of developmental transitions: lessons from *Drosophila* research. Annu. Rev. Entomol. ***58***: 497–516. https://doi.org/10.1146/annurev-ento-120811-153608.
43. Sun, W., Shen, Y.H., Qi, D.W., et al. (2012). Molecular cloning and characterization of ecdysone oxidase and 3-dehydroecdysone-3α-reductase involved in the ecdysone inactivation pathway of silkworm, *Bombyx mori*. Int. J. Biol. Sci. ***8***(1): 125–138. https://doi.org/10.7150/ijbs.8.125.
44. Takeuchi, H., Rigden, D.J., Ebrahimi, B., et al. (2005). Regulation of ecdysteroid signalling during *Drosophila* development: identification, characterization and modelling of ecdysone oxidase, an enzyme involved in control of ligand concentration. Biochem. J. ***389***: 637–645. https://doi.org/10.1042/Bj20050498.
45. Takeuchi, H., Chen, J.H., O'Reilly, D.R., et al. (2001). Regulation of ecdysteroid signaling: cloning and characterization of ecdysone oxidase: a novel steroid oxidase from the cotton leafworm, *Spodoptera littoralis*. J. Biol. Chem. ***276***(29): 26819–26828. https://doi.org/10.1074/jbc.M104291200.
46. Guittard, E., Blais, C., Maria, A., et al. (2011). CYP18A1, a key enzyme of *Drosophila* steroid hormone inactivation, is essential for metamorphosis. Dev. Biol. ***349***(1): 35–45. https://doi.org/10.1016/j.ydbio.2010.09.023.
47. Sommé-Martin, G., Colardeau, J., and Lafont, R. (1988). Conversion of ecdysone and 20-hydroxyecdysone into 3-dehydroecdysteroids is a major pathway in third instar *Drosophila melanogaster* larvae. Insect Biochem. ***18***(7): 729–734. https://doi.org/10.1016/0020-1790(88)90082-0.
48. Kang, S., Sun, D., Qin, J.Y., et al. (2022). Fused: a promising molecular target for an RNAi-based strategy to manage Bt resistance in *Plutella xylostella* (L.). J. Pest. Sci. ***95***(1): 101–114. https://doi.org/10.1007/s10340-021-01374-3.

ACKNOWLEDGMENTS

We thank Prof. David G. Heckel from the Max Planck Institute for Chemical Ecology for his constructive comments on a draft of this manuscript, and we also thank Prof. Xia Cui and Dr. Haijing Wang from our institute for the assistance with the UPLC-MS/MS experiment. This work was supported by the National Natural Science Foundation of China (32221004, 32172458, and 32372600), the China Postdoctoral Science Foundation (2023M733828), the earmarked fund for CARS (CARS-23), the Central Public-interest Scientific Institution Basal Research Fund (Y2024XK01), the Beijing Key Laboratory for Pest Control and Sustainable Cultivation of Vegetables, and the Innovation Program of Chinese Academy of Agricultural Sciences (CAAS-CSCB-202303).

AUTHOR CONTRIBUTIONS

Conceptualization, Z.G., L.Z., N.C., and Y.Z.; investigation, Z.G., L.Z., Z.C., L.D., L.G., Y.B., Q.W., S.W., X.Y., W.X., and N.C.; methodology, Z.G., L.Z., Z.C., L.D., L.G., Y.B., and N.C.; funding acquisition, Z.G., L.Z., and Y.Z.; writing – original draft, Z.G., L.Z., L.D., and N.C.; writing – review & editing, Z.G., L.Z., N.C., X.Z., R.L., and Y.Z.

DECLARATION OF INTERESTS

The authors declare no competing interests.

SUPPLEMENTAL INFORMATION

It can be found online at https://doi.org/10.1016/j.xinn.2024.100675.

LEAD CONTACT WEBSITE

http://www.ivfcaas.ac.cn/rck/zyj/256646.htm
https://ivf.caas.cn/en/PEOPLE/Professor/1b35953491ab414692e0420a5a09be32.htm.